Symmetry character of bands in $^{72-84}$Kr in the proton-neutron interacting boson model

A. Giannatiempo and P. Sona
Dipartimento di Fisica, Università di Firenze e Istituto Nazionale di Fisica Nucleare, Sezione di Firenze, Florence, Italy

A. Nannini
Istituto Nazionale di Fisica Nucleare, Sezione di Firenze, Florence, Italy

(Received 8 July 1999; published 28 August 2000)

The positive-parity bands observed in the even $^{72-84}$Kr isotopes have been studied in the framework of the IBA-2 model. The analysis includes states of spin up to the maximum allowed by the finite boson number. The symmetry character of these bands in the proton and neutron degrees of freedom has been investigated. Excitation energies, $B(E2)$'s of intraband transitions and $B(E2)$'s, $B(M1)$'s, $E2/M1$ mixing ratios of interband transitions have been considered. Three bands of different structure can be accounted for in the framework of the model: the ground-state band, of predominant full-symmetry character; the band built on the 2_2^+ state, which is composed by states which show different symmetry character along the isotopic chain; and the band built on the 3_1^+ state, of predominant mixed-symmetry character.

PACS number(s): 21.60.Fw, 21.10.Re, 27.50.+e

I. INTRODUCTION

In nuclear structure studies the concept of mixed-symmetry (MS) states, i.e., of states not completely symmetric in the proton and neutron degrees of freedom, arises naturally when distinction is made between the two types of nucleons. A 1^+ scissors mode was predicted in deformed nuclei by Lo Iudice and Palumbo [1] in the framework of the two-rotor model and by Iachello [2] in the framework of the IBA-2 model [3]. Clear experimental evidence for the presence of MS states came in the early 1980s with the identification of the 1^+ MS state in ^{156}Gd via inelastic electron scattering experiments [4].

In the following years the 1^+ scissors modes have been studied systematically in different mass regions (see, e.g., [5,6]) whereas experimental information on low-lying MS states in vibrational nuclei (in which the lowest MS state has $J^\pi = 2^+$) is still rather fragmentary (see, e.g., [7–11]). Very recently Pietralla *et al.* [12] have observed, in addition to the 2^+ MS state, the 1^+ MS state in the gamma instable nucleus ^{94}Mo.

In an attempt to identify as many MS states as possible in nuclei of vibrational type, we have performed in the last few years a systematic phenomenological study in the $A=100$ mass region. We have analyzed the isotopes ^{110,112,114}Cd ($Z=48$) [13,14], $^{100-116}$Pd ($Z=46$) [15,16], and $^{98-114}$Ru ($Z=44$) [16,17] in the framework of the IBA-2 model. In this model the degree of symmetry of a state is related to its F-spin value. In the well-known limiting cases, where the F-spin is a good quantum number, fully symmetric (FS) states are characterized by the eigenvalue $F=F_{max}=N/2$ (where N is the total number of bosons) while MS states are characterized by $F=F_{max}-1, F_{max}-2$, etc.

As a result of the analyses of the Cd, Pd, and Ru chains (which consider energies, electromagnetic moments, and decay properties) groups of positive-parity states of predominant $F=F_{max}-1$ character were identified and several indications for the presence of $F<F_{max}-1$ states were pointed out. Besides, a restricted range of viable values for the Majorana parameters ξ_2 and ξ_3, for which no indication is available from microscopic considerations, was determined for the $A\simeq 100-120$ mass region.

In this work we consider the even $^{72-84}$Kr isotopes ($Z=36$). They have been extensively studied both experimentally and theoretically and it has been found that, in addition to collective excitations, other degrees of freedom such as shape coexistence at low spins (see, e.g., [18,19]), two-quasiparticle aligned configurations (see, e.g., [20,21]), etc., can take part in determining excitation-energy patterns and decay properties.

Our aim was to investigate to what extent the IBA-2 model is able to describe positive-parity bands in these isotopes when states up to the maximum spin allowed by the finite boson number are considered and, at the same time, to check whether the role played by states of MS character in determining the properties of nuclei in the $A\simeq 80$ mass region is as important as in the $A\simeq 100-120$ mass region. The analysis we carried out some time ago [22] on low-lying states in ^{78,80,82}Kr has been used as a starting point.

The first systematic analysis of even krypton isotopes in the framework of the IBA-2 model was performed a long time ago by Kaup and Gelberg [23] who considered the energy spectra (up to $J=6$) and the decay properties of the 2_2^+ state in $^{74-82}$Kr. Recently, another systematic study of low-lying states in $^{72-84}$Kr have been performed by Dejbakhsh *et al.* [24]. These authors, starting from the parameters reported in [22], analyzed the energy spectra up to $J=8$ and $B(E2)$ ratios of transitions connecting low-lying states. Studies based on the IBA-2 model, limited to specific krypton isotopes, have been reported in [25–27].

II. PARAMETERS OF THE IBA-2 MODEL

For the present calculations we used the same Hamiltonian as in our previous works [15–17], namely,

$$H=\varepsilon\,(\hat{n}_{d_\pi}+\hat{n}_{d_\nu})+\kappa\,\hat{Q}_\pi^{(\chi_\pi)}\cdot\hat{Q}_\nu^{(\chi_\nu)}+w_{\pi\nu}\hat{L}_\pi\cdot\hat{L}_\nu+\hat{M}_{\pi\nu}. \quad (1)$$

The four terms represent the d-boson energies (which for simplicity has been taken equal for proton and neutron bosons), the π-boson, ν-boson quadrupole and dipole interactions and the Majorana operator, respectively. The $\hat{L}_\pi \cdot \hat{L}_\pi$ operator, present in the Hamiltonian used in our previous work on $^{78-82}$Kr, was not included in Eq. (1) to reduce as much as possible the number of model parameters. We used the generalized Majorana operator [28], whose expression is given by

$$\begin{aligned}\hat{M}_{\pi\nu} = & \tfrac{1}{2}\,\xi_2[s_\nu^\dagger \times d_\pi^\dagger - s_\pi^\dagger \times d_\nu^\dagger]^{(2)} \cdot [\tilde{s}_\nu \times \tilde{d}_\pi - \tilde{s}_\pi \times \tilde{d}_\nu]^{(2)} \\ & + \xi_1[d_\nu^\dagger \times d_\pi^\dagger]^{(1)} \cdot [\tilde{d}_\nu \times \tilde{d}_\pi]^{(1)} \\ & + \xi_3[d_\nu^\dagger \times d_\pi^\dagger]^{(3)} \cdot [\tilde{d}_\nu \times \tilde{d}_\pi]^{(3)}, \end{aligned} \tag{2}$$

where the parameters ξ_1, ξ_2, ξ_3 can take independent values.

In the IBA-2 model the $E2$ and $M1$ operators are expressed as [3]

$$\hat{T}(E2) \equiv e_\nu \hat{T}_\nu(E2) + e_\pi \hat{T}_\pi(E2) = e_\nu \hat{Q}_\nu^{(\chi_\nu)} + e_\pi \hat{Q}_\pi^{(\chi_\pi)}, \tag{3}$$

$$\begin{aligned}\hat{T}(M1) \equiv & g_\nu \hat{T}_\nu(M1) + g_\pi \hat{T}_\pi(M1) \\ = & \sqrt{\frac{3}{4\pi}}(g_\nu \hat{L}_\nu + g_\pi \hat{L}_\pi), \end{aligned} \tag{4}$$

where e_ρ and g_ρ ($\rho = \pi, \nu$) are the effective quadrupole charges and gyromagnetic ratios, respectively. The values of χ_ρ are the same as in the Hamiltonian (consistent-Q formalism). Altogether 12 parameters are present in expressions (1)–(4).

Calculations have been performed by using the NPBOS code [29] which includes, as outputs, the decomposition of the wave function of each state in terms of the number of d-boson, n_d, and of the F-spin components.

The procedure followed to fix the parameters $\varepsilon, \kappa, w_{\pi\nu}$ is the same as described in [22]. The values of χ_π and χ_ν have been kept fixed along the isotopic chain to the same value ($\chi_\pi = -0.1$, $\chi_\nu = -1.1$) deduced for $^{78-82}$Kr in [22].

As to the Majorana parameters, the value of ξ_2 has been determined taking into account the possible influence of this parameter on the experimental energies as well as on the decay properties of all the states. The $E2/M1$ mixing ratios proved to be particularly useful in fixing its value. The value of ξ_3 has been adjusted, basically, so as to reproduce the energies of odd-spin states.

For the parameter ξ_1 we chose a value sufficiently high to move the lowest 1^+ MS state at an energy $\geqslant 2$ MeV; this is justified by the absence of any $J^\pi = 1^+$ level unambigously established below this energy. We have also checked that the calculated excitation energies of the levels relevant to this work are quite insensitive to the value of ξ_1.

As to the effective quadrupole charges we adopted the values derived in [22], namely $e_\pi = 0.075$, $e_\nu = 0.090$ e b. Their values are rather close to those we found in the ruthenium ($e_\pi = 0.080$, $e_\nu = 0.120$ e b) and palladium ($e_\pi = 0.095$, $e_\nu = 0.115$ e b) chains. Also the values of the gyromagnetic ratios ($g_\pi = 0.70$, $g_\nu = 0.40$ μ_N) are the same as in [22]. They are slightly higher than those adopted in the palladium and ruthenium chains ($g_\pi = 0.51$, $g_\nu = 0.28$ μ_N) but the difference $g_\pi - g_\nu$, which appears as a factor in the expression of the $M1$ strength, is similar in the two cases.

TABLE I. Adopted values for the Hamiltonian parameters used for IBA-2 calculations. All parameters are given in MeV. The values of the parameters kept fixed along the isotopic chain are $\chi_\pi = -0.1$, $\chi_\nu = -1.1$ (dimensionless), and $\xi_1 = 1.1$ MeV. The values of the ξ_2, ξ_3 in ^{72}Kr are reported in italics since, their determination not being possible on the basis of the available experimental data, they have been kept equal to those in ^{74}Kr.

A	ε	κ	$w_{\pi,\nu}$	ξ_2	ξ_3
72	0.930	−0.085	0.010	*−0.030*	*0.200*
74	0.835	−0.090	0.020	−0.030	0.200
76	0.830	−0.095	0.025	−0.030	0.120
78	0.800	−0.095	0.020	0.00	0.050
80	0.880	−0.085	0.020	0.140	−0.060
82	1.000	−0.085	0.020	0.170	−0.200
84	1.050	−0.085	0.020	0.240	−0.220

The values of the parameters varied along the isotopic chain are reported in Table I. In ^{72}Kr the available

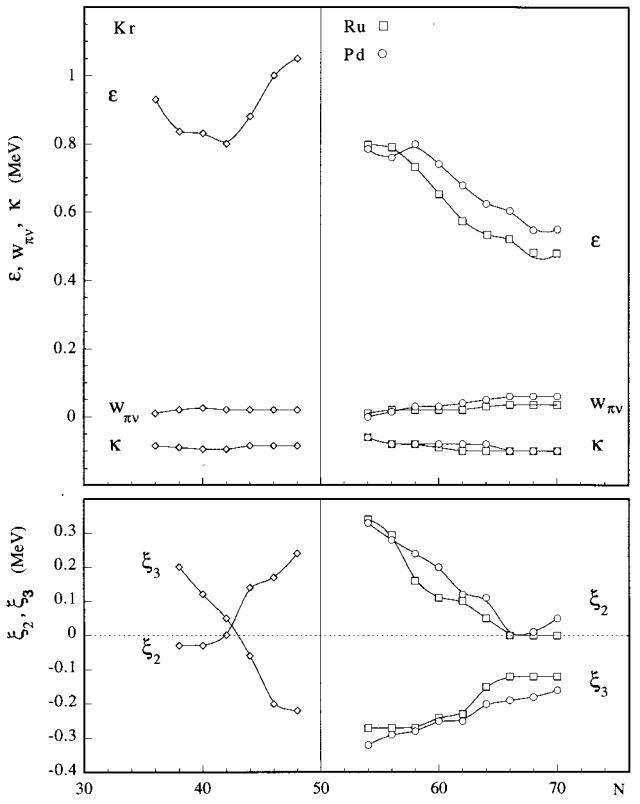

FIG. 1. The adopted values of the Hamiltonian parameters which have been varied along the krypton chain are shown, as a function of the neutron number, on the left-hand side of the figure. The values of the same parameters for the palladium [15] and ruthenium [17] chains are also reported for comparison.

experimental data do not allow us to estimate the values of ξ_2, ξ_3, which have thus been kept equal to those in ^{74}Kr.

As can be seen from the table, the parameters κ and $w_{\pi,\nu}$ have a very limited range of values so that there are essentially only three parameters $(\varepsilon, \xi_2, \xi_3)$ which exhibit a large variation along the isotopic chain.

It is interesting to compare (see Fig. 1) the behavior of the parameters reported in Table I with that of the corresponding ones in the Pd and Ru chains as a function of the neutron number. In both neutron major shells (28–50) and (50–82) the trend is similar for $\varepsilon, \kappa, w_{\pi,\nu}$: ε decreases in moving towards the middle of the neutron shell while both κ and $w_{\pi,\nu}$ stay approximately constant and have similar values in the three isotopic chains.

As to the Majorana parameters, we can observe that the value of ξ_2 decreases monotonically in going from the beginning of the neutron shell towards the middle of the shell in the Pd and Ru chains and that it increases monotonically from the middle towards the end of the shell in the Kr chain. Such a trend suggests a similar behavior of this parameter in the two neutron major shells, i.e., large and positive values near closed neutron shells and minimum value at the middle of the shell. The values of ξ_2 become rather close in the two major shells when the neutron number approaches 50 and this is also the case for ξ_3. Until now no explanation based on microscopic studies has been provided for the Majorana term in its full generality so that we do not have an interpretation for the trend determined phenomenologically for ξ_2 and ξ_3.

As a final remark, we note that for large values of the ratio ε/κ and small values of the boson number, the *d*-boson energy term in the Hamiltonian becomes predominant. This is the case for the heavy krypton isotopes for which the calculations predict a structure rather close to the U(5) limit of the IBA-2 model.

III. RESULTS AND DISCUSSION

To investigate whether among the bands observed in $^{72-84}$Kr there are some of predominant FS or MS character it has been useful to refer to the groups of states shown in Fig. 2, which are the eigenstates of the simple U(5) invariant

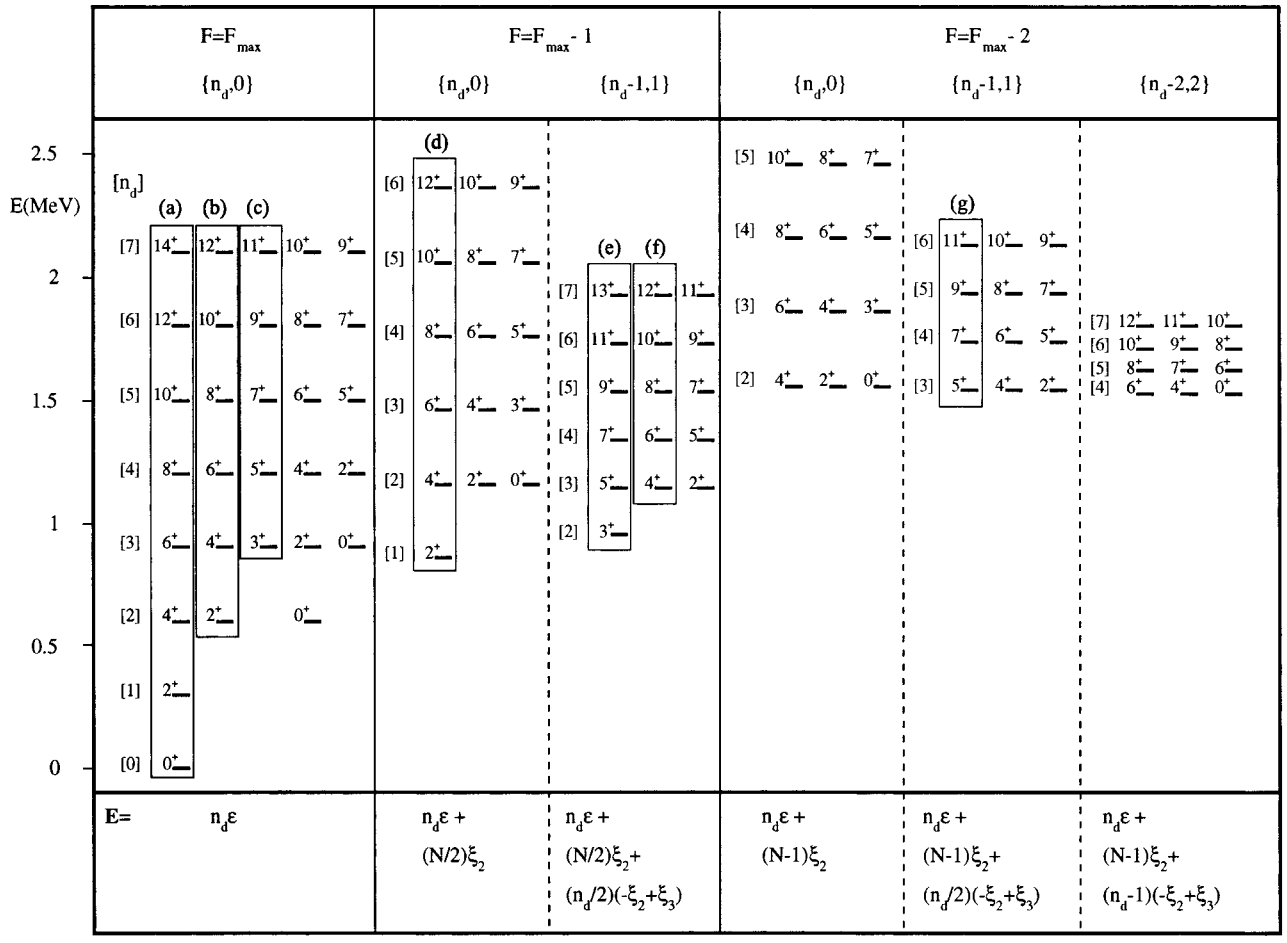

FIG. 2. Eigenstates of the U(5) Hamiltonian $H=\varepsilon\,(\hat{n}_{d_\pi}+\hat{n}_{d_\nu})+M_{\pi\nu}(\xi_1,\xi_2,\xi_3)$ for the particular case $N=7$. Fully symmetric states are displayed together with $F=F_{max}-1$ and $F=F_{max}-2$ states whose energy does not depend on the parameter ξ_1. States are separated in three sections labeled by the *F*-spin quantum number. MS states are reported in separated columns according to their different dependence on the Majorana parameters ξ_2 and ξ_3, given at the bottom. At the top of each column are shown the quantum numbers $\{n_1, n_2\}$ of the relevant $U_{\nu+\pi}(5)$ representation. On the left of each degenerate multiplet the number of *d*-bosons is reported in square brackets. The subsets of states of particular interest to the discussion have been enclosed in a frame and marked by a letter.

Hamiltonian $H=\varepsilon(\hat{n}_{d_\pi}+\hat{n}_{d_\nu})+M_{\pi\nu}$. The figure summarizes the results reported in [15,16,30], concerning the excitation energies of MS states whose Majorana operator eigenvalues depend only on ξ_2 and ξ_3. These states are reported in five separate columns according to the expressions obeyed by their energy eigenvalues, which are given in the lower part of the figure. In the first column are reported the FS states. States in each column belong to degenerate multiplets characterized by the number of d bosons; for a given n_d only the five FS and the three MS states of highest spin are shown. Mixed-symmetry states having $\{n_d,0\}$ quantum numbers are the counterpart of the FS states and the $F_{max}-2$, $\{n_d-1,1\}$ states are the counterpart of the $F_{max}-1$, $\{n_d-1,1\}$ states. Subsets of states enclosed in a frame will be referred to as ''band'' in the following. They correspond to the bands present in the calculated spectrum when the degeneracy of levels of the same multiplet is lifted by using a general U(5) Hamiltonian (see, e.g., Fig. 2.1 in [3]). To help the reader in the following discussion they are marked by letters whereas bands in krypton isotopes calculated by means of the realistic Hamiltonian (1) (and the associated experimental ones) are marked by numbers.

In the spectrum of a nucleus having a structure not too far from the U(5) limit one could expect to observe, in addition to the ground-state (g.s.) band (of FS character) two bands built on a 2^+ state, corresponding to bands (b) and (d), and two bands built on a 3^+ state, corresponding to bands (c) and (e). States of the same spin in bands (b),(d) and (c),(e) have different decay properties due to their different F spin and n_d values. For example, states of band (d) can decay via an $M1$ transition (which obeys the selection rule $\Delta n_d=0$) to states of the same J in band (a) while, obviously, this is not the case for states of band (b). When a realistic Hamiltonian is used, calculations can predict that states of the same spin in the two pairs of bands be rather close in energy and share therefore their properties.

Important hints for the identification of a band having MS character are provided by the following.

(i) Capability of the calculations to reproduce the excitation energy of states in the band by a suitable choice of the Majorana parameters.

(ii) Large $M1$ components in transitions connecting MS candidates with $F=F_{max}-1$ to states having FS character [$M1$ transitions are forbidden between $F=F_{max}$ states and in the U(5) limit, satisfy the $\Delta F=0,\pm1$ selection rule [31,7]].

(iii) Hindered $E2$ transitions connecting states of an MS band to states of an FS band. Small values of the $E2/M1$ mixing ratio δ can provide therefore important signatures for the identification of MS states.

(iv) Large $E2$ transitions connecting states in a given MS band, comparable in magnitude with those connecting states in a FS band.

The comparison of experimental and calculated data in $^{72-84}$Kr is shown in Figs. 3–10. Some predicted states not having the corresponding experimental ones are also shown

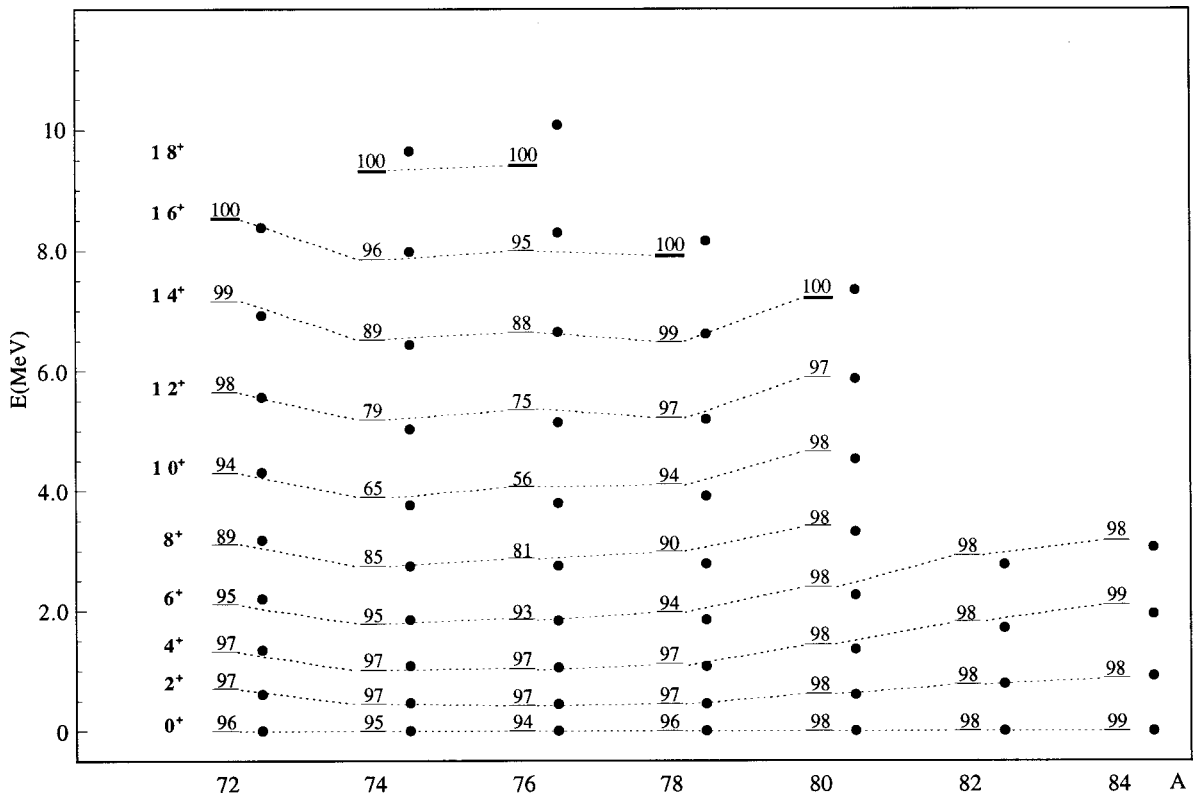

FIG. 3. Experimental excitation energies (horizontal lines) of states identified as belonging to bands (1) (see text) in the krypton chain are compared to the calculated values (dots). The number reported above each line gives the percentual square amplitude of the F_{max} component of the state.

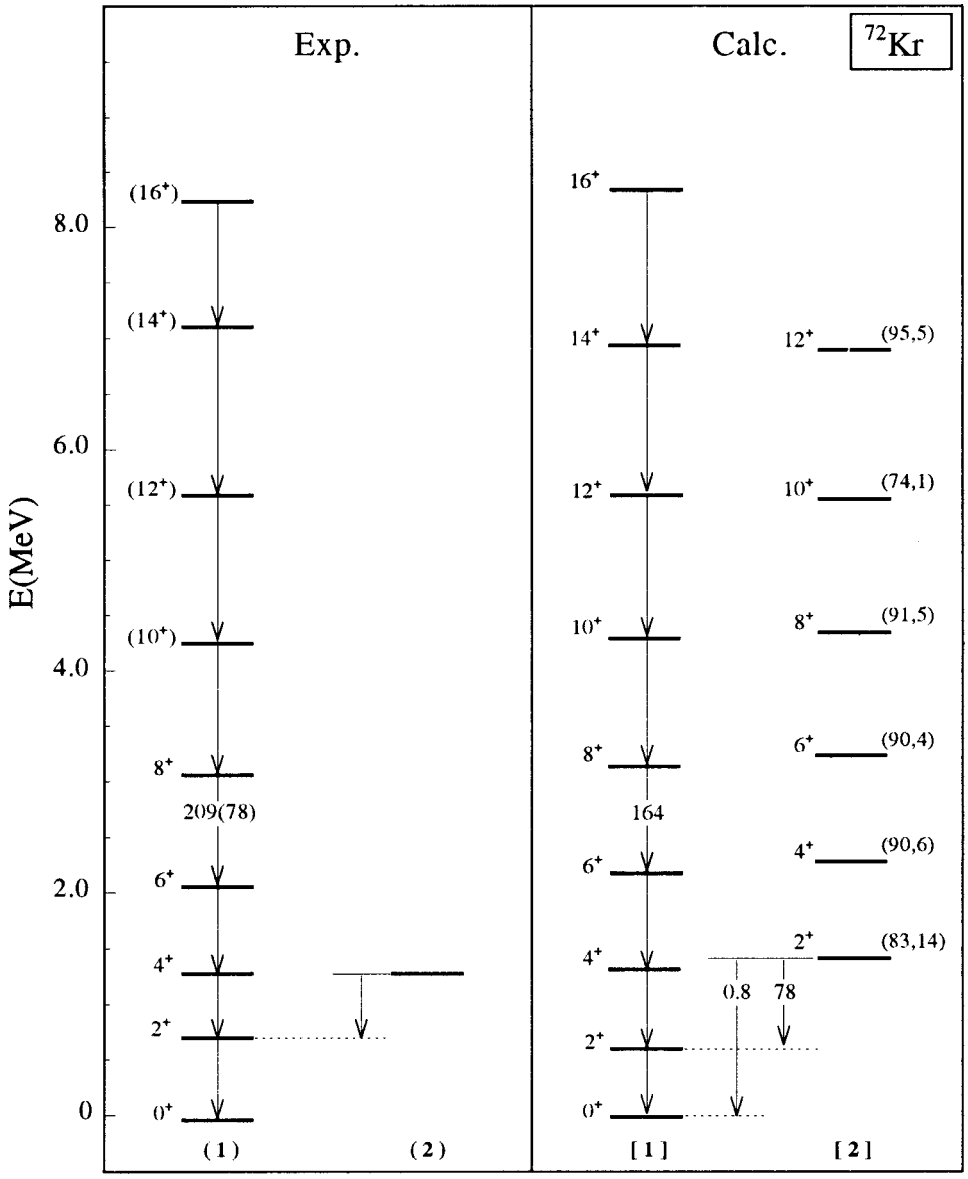

FIG. 4. Experimental energies of the levels belonging to g.s. band in ^{72}Kr and the only known $B(E2)$ value (of the $8^+ \rightarrow 6^+$ transition, in units of $10^{-3}e^2$ b^2) are compared to the calculated ones. Also shown is the predicted second excited 2^+ state, of full-symmetry character, which can possibly be associated to the experimental level at 1.316 MeV.

in Figs. 4–8 and 10. Experimental data are taken from the following references: ^{72}Kr [32], ^{74}Kr [33–35], ^{76}Kr [36–38], ^{78}Kr [26,39,40], ^{80}Kr [21,41], ^{82}Kr [42,43], and ^{84}Kr [44].

In the fitting procedure for the determination of the model parameters the 2_1^+ state in ^{72}Kr (whose ''high'' energy is most likely related to shape coexistence) and the states of spin $J \geqslant 12$ in ^{74}Kr and $J \geqslant 10$ in ^{74,76,78}Kr (where an upbending is apparent) have not been considered.

For the sake of clarity, $B(M1)$ values are enclosed in a box while $E2/M1$ mixing ratios and predominant multipolarity of the transitions are shown in the up-down direction. A dashed horizontal line has been used to indicate an experimental state not definitely identified or a predicted state for which the correspondence with the experimental one is not well established.

Bands having similar structure in the different isotopes are labeled by the same number which is reported in parentheses for experimental bands and in square brackets for the corresponding calculated bands. In Figs. 4–10 the percentual values of $\alpha^2(F_{max})$ and $\alpha^2(F_{max}-1)$ are reported in parentheses next to each level of band [2].

For completeness, we also report the states (dotted lines) of the band observed in ^{74,76,80}Kr, built on a 8^+ state at about 3.5 MeV, which in ^{74,80}Kr has been interpreted as due to quasi-particle excitations (see, e.g., [34,21]).

A. Band (1)

Band (1) is composed of the even-spin yrast states in all isotopes, except for the $10_2^+, 12_2^+, 14_2^+$ states in ^{80}Kr [21]. The experimental energies (horizontal lines) of the states belonging to band (1) are shown together with the calculated

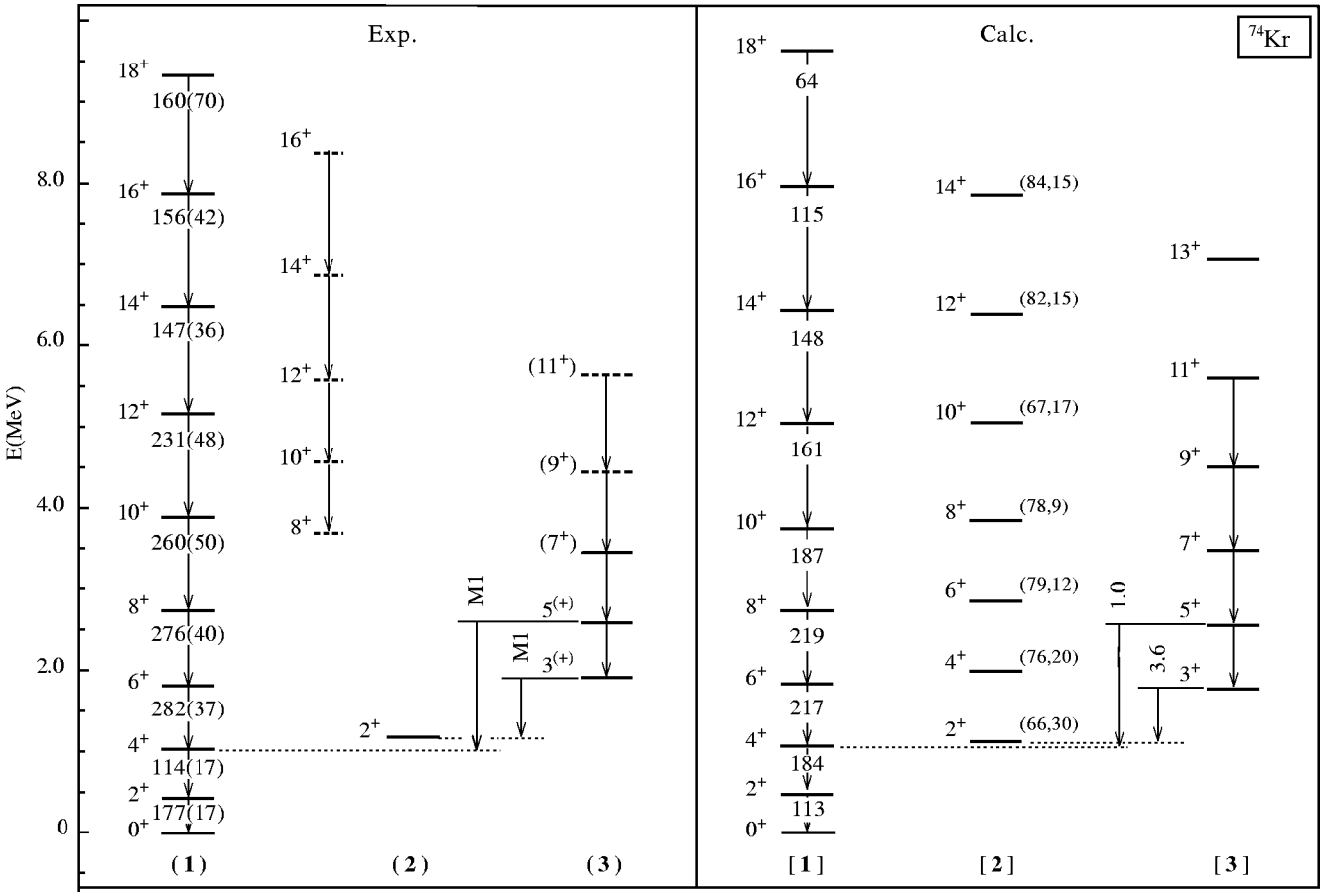

FIG. 5. Comparison of experimental and calculated energies, $B(E2)$ values (in units of $10^{-3}e^2$ b^2) of intraband transitions and $E2/M1$ mixing ratios (vertical writing) of interbands transitions in ^{74}Kr. The band built on the 8^+ state, whose states are represented by dotted lines, is outside the IBA-2 model space.

ones (dots) in Fig. 3. Above each line is reported the percentage (amplitude square, α^2) of the F_{max} component of the state.

In $^{72-80}$Kr the comparison is possible up to the state (indicated by a thick horizontal line) having the maximum spin allowed by the total boson number. In ^{82,84}Kr band (1) is recognizable only up to the $J=6$ state because at higher energies the spectrum looks quite complicated due to excitations of noncollective degrees of freedom [43].

The experimental excitation energies vary smoothly along the isotopic chain, as expected for collective states, and are reproduced, on the average, to an accuracy of a few percent. It is to be noted that the average accuracy of the high-spin states not utilized in the fitting procedure is about 2% for ^{74,78,80}Kr and about 4% for ^{76}Kr, respectively.

As to the decay properties, it turns out that the $B(E2)$ values of the transitions in band (1) are rather well reproduced along the isotopic chain (see Figs. 4–10), including the cases in which the comparison can be extended to transitions connecting high-spin states in the band (^{74,78}Kr).

In ^{82,84}Kr the calculations largely overestimate the $B(E2;6^+\rightarrow 4^+)$ (see Figs. 9 and 10) so that, in spite of the good agreement between experimental and calculated energies, it seems difficult to identify the 6_1^+ state in these isotopes as a member of band (1). This conclusion is in agreement with what is found in [43].

It is seen from Fig. 3 that states of band [1] have a quite pure FS character, with $\alpha^2(F_{max})\geqslant 0.90$ (the few exceptions will be discussed in Sec. III B). In all isotopes the largest n_d component (n_{dm}) of a state of given J is just that characterizing the state J in column (a). Its amplitude square $\alpha^2(n_{dm})$ increases, in each isotope, from low- to high-spin states and, along the isotopic chain, in moving away from the neutron midshell.

In the lighter isotopes several n_d components are present in the wave functions of the states of band [1] [which suggests a structure close to the O(6) limit, where n_d is no longer a good quantum number], the value of $\alpha^2(n_{dm})$ still being higher than $\simeq 0.6$. In ^{82,84}Kr, where $\alpha^2(n_{dm})$ is $\geqslant 0.93$, the structure of band [1] is quite close to that of band (a), i.e., to that of the U(5) limit.

A change in the structure from O(6) to U(5) for increasing atomic mass, already pointed out in [27], is consistent with the trend of the experimental ratios $B(E2;J\rightarrow J-2)/B(E2;2_1^+\rightarrow 0_1^+)$. They are reported in Fig. 11 together with those calculated in the limits of the model: in the lighter isotopes the ratios match both the O(6) and the SU(3) limits while they become compatible with those of the U(5) limit moving towards the heavier ones.

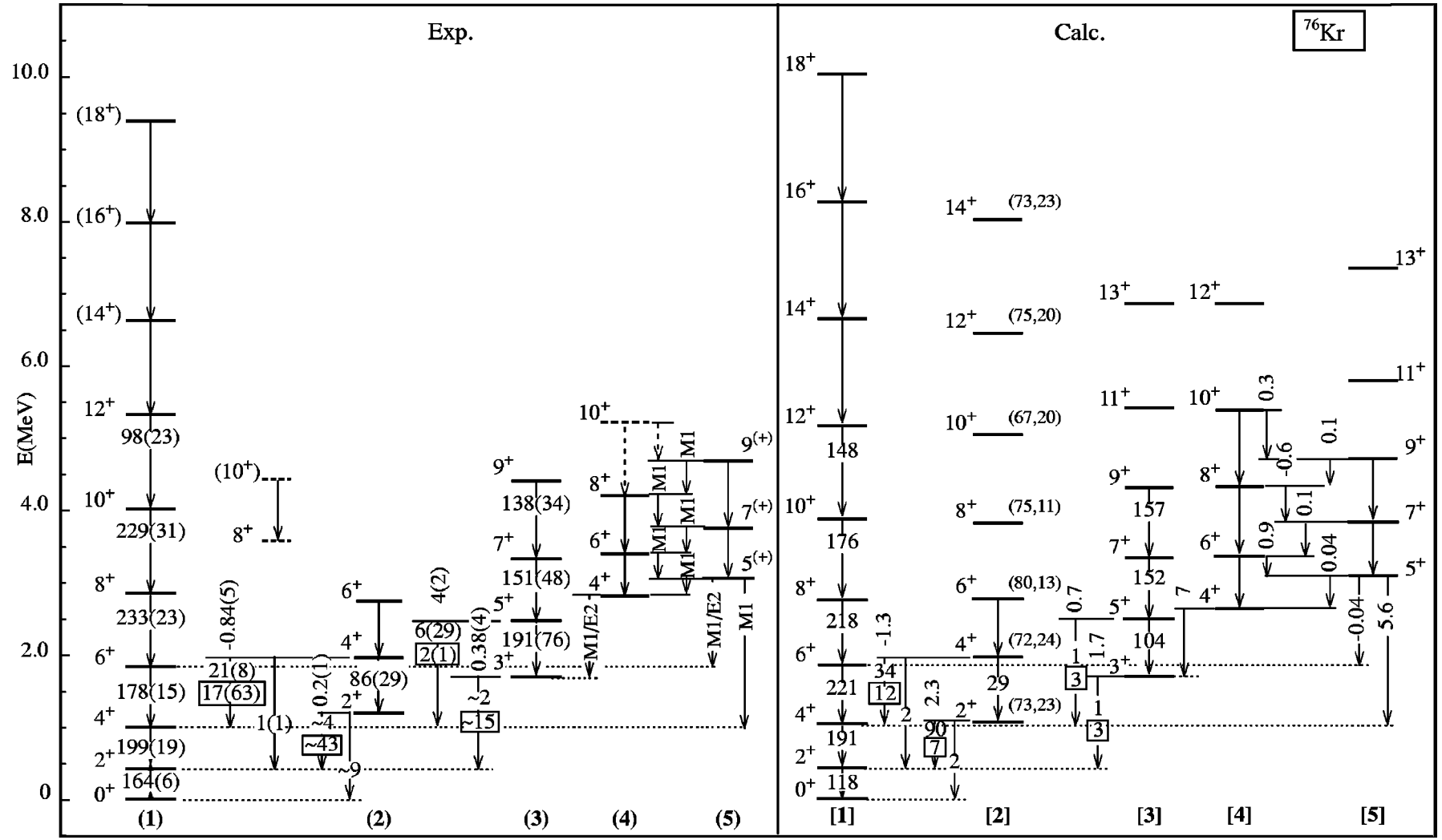

FIG. 6. Comparison of experimental and calculated energies, $B(M1)$ values (enclosed in a box, in units of $10^{-3}\mu_N^2$), $B(E2)$ values (in units of $10^{-3}e^2$ b^2), and $E2/M1$ mixing ratios (vertical writing) in ^{76}Kr. The numbers attached to the horizontal lines representing the states in band [2] give the calculated percentual intensity of the $F=F_{max}$ and $F_{max}-1$ components. The band built on the 8^+ state is outside the IBA-2 model space.

044302-7

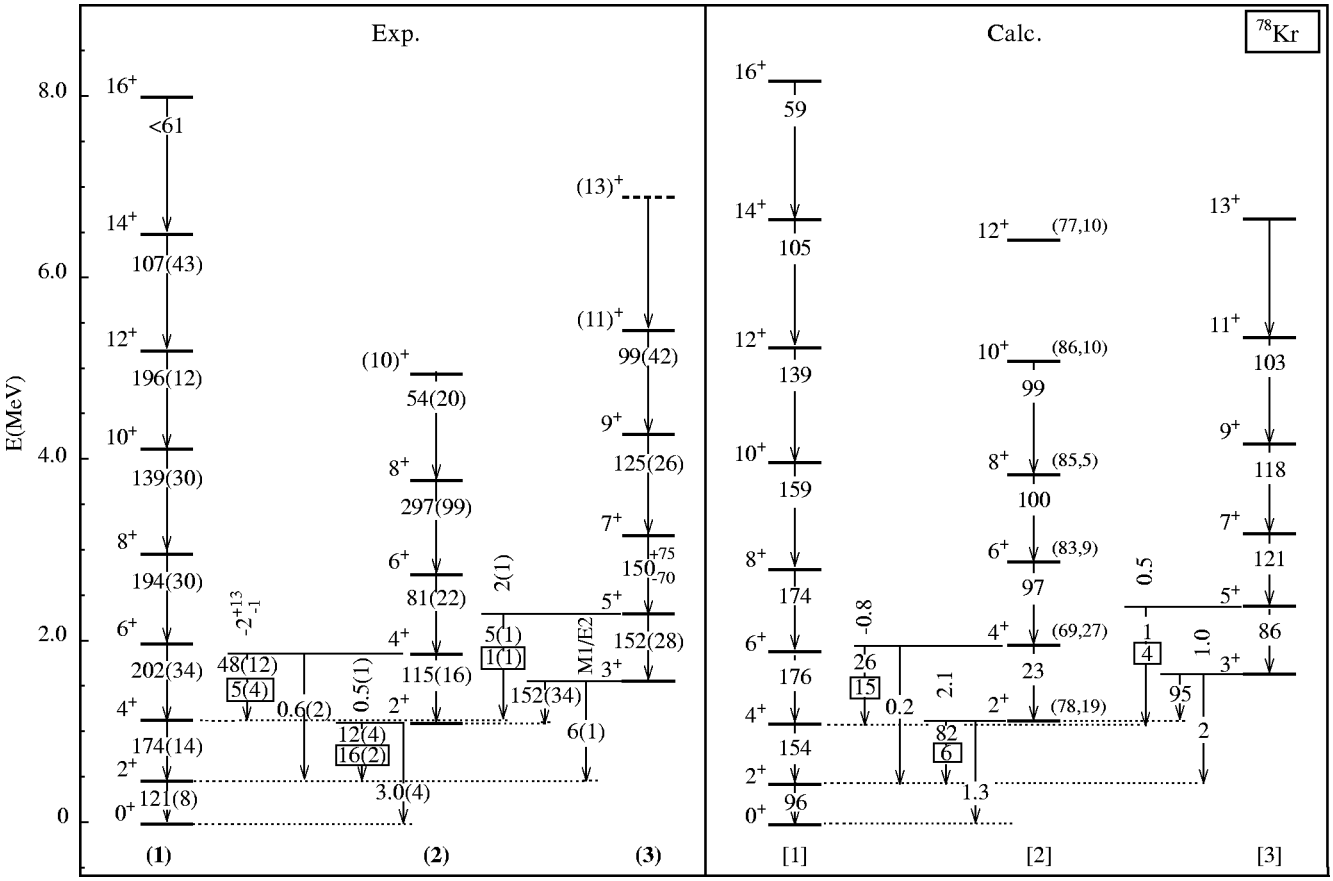

FIG. 7. As in Fig. 6, for ^{78}Kr.

B. Band (2)

Band (2) is built on the 2_2^+ state. This state has been identified or proposed in all isotopes with the only exception of ^{72}Kr where, however, it has probably to be identified (see also Fig. 4) with the level at 1.316 MeV, which is very close in energy to the 4_1^+, 1.321 MeV state. Levels of higher spin belonging to this band have been observed in $^{76-82}$Kr. A noticeable feature of this band is the presence of an important $M1$ component in the transitions connecting the 2^+ and 4^+ states to the states of the same spin of band (1) (see Figs. 6–10).

The calculations predict in each isotope a band of FS character having a structure rather close to that of band (b) and a band of MS character having a structure rather close to that of band (d) in Fig. 2. The values of ξ_2, whose choice proved to be essential for a close matching of the spectroscopic experimental data, have only a minor effect on the energies of the states of the former band and a strong one on those of the latter.

On the whole the calculations predict reasonably well energies and $B(E2)$'s of intraband transitions as well as $B(E2)$ and $B(M1)$ values of interband transitions and reproduce the sign of δ (the Krane and Steffen [45] phase convention has been used).

Because $M1$ transitions are forbidden between $F=F_{max}$ states, the possibility of reproducing the properties of the interband transitions rests on a correct evaluation of the MS components in the wave functions of the relevant states. From the values of $\alpha^2(F_{max})$ and $\alpha^2(F_{max}-1)$ the following is seen.

(i) In ^{76,78}Kr states of band [2] have essentially FS character; at the same time, the 2^+ and 4^+ states of the calculated bands of FS and MS character are predicted to be sufficiently close in energy to partially share their character. Since the structure of band [2] is close to that of band (b) the predominant n_d component of a state of spin J in band [2] is the same as that of the state of spin $J+2$ of band [1]. The corresponding states of spin $J+2$ and J and in the experimental bands (1) and (2) are rather close in energy, as can be clearly seen in the spectrum of ^{78}Kr where band (2) extends high in energy. It seems therefore possible to consider these pairs of states as members of the same n_d multiplet. In ^{76}Kr the calculations predict also an influence of the MS band on the properties of band [1] when levels of equal J are close in energy, such as the 10^+ level of the MS band and that of the g.s. FS band. This gives rise to a low value (0.56) of $\alpha^2(F_{max})$ for the 10_1^+ state. A smaller mixing is predicted for the 8^+ and for the 12^+ state of the two bands. Similar considerations apply to the corresponding states in ^{74}Kr.

(ii) In ^{80}Kr the calculations predict the crossing of the band of MS character and of FS character between $J=4$ and $J=6$ (see Fig. 8). The calculated $B(E2;6^+\rightarrow 4^+)$ is rather large and compares well with the experimental one. For the 2^+ and 4^+ states the same observations made for ^{76,78}Kr apply.

(iii) In ^{82}Kr the crossing of the two bands happens at a lower spin value (between $J=2$ and $J=4$) and also in this

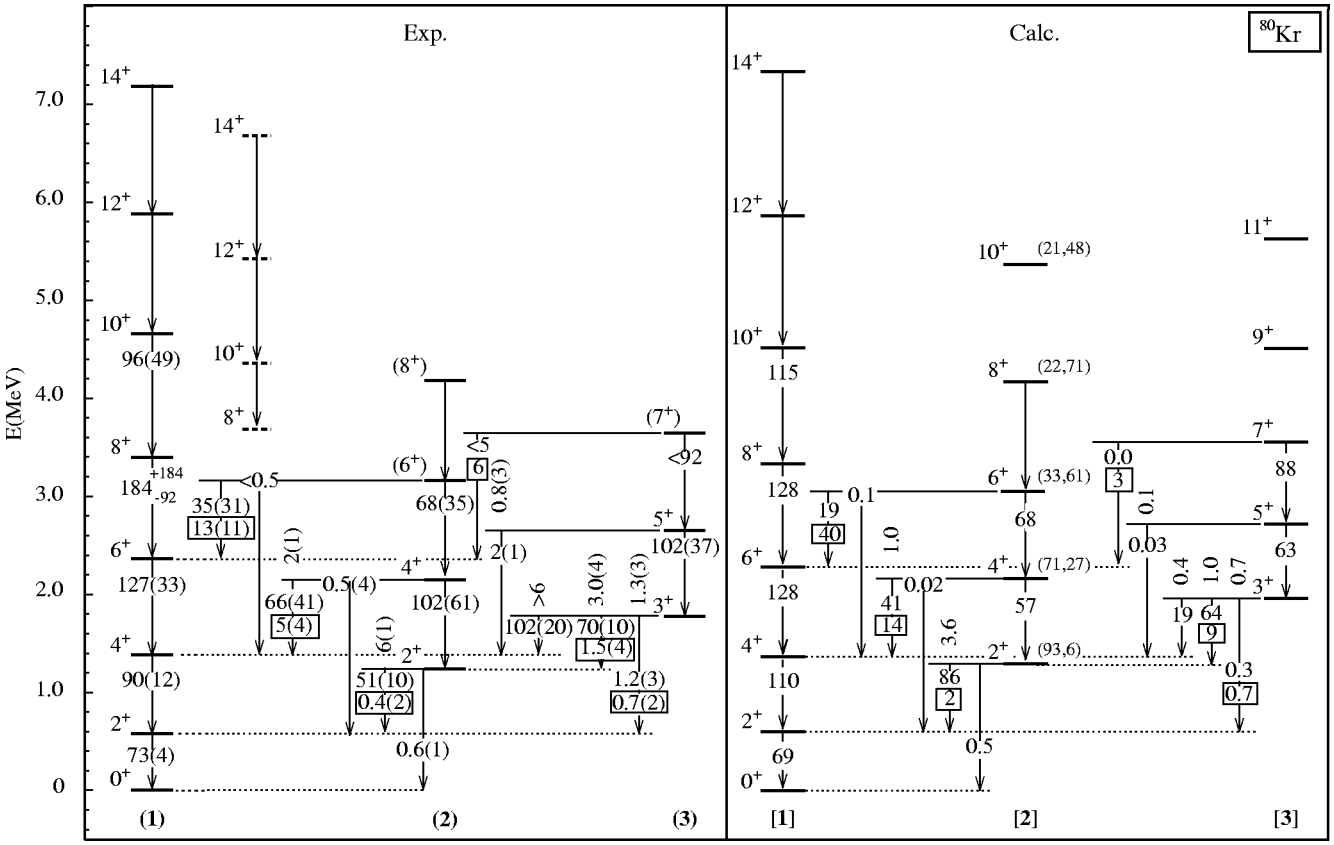

FIG. 8. As in Fig. 6, for ^{80}Kr. The experimental and calculated $B(E2)$ and $B(M1)$ values of the $6_2^+ \rightarrow 6_1^+$ and $7_1^+ \rightarrow 6_1^+$ transitions are those evaluated for a transition of pure $E2$ or $M1$ multipolarity.

case the calculations reproduce correctly the value of the $B(E2;4^+ \rightarrow 2^+)$.

(iv) In ^{84}Kr only the 2_2^+ state can be identified as belonging to band (2). It has a predominant MS character (see Fig. 10) with a large $n_d=1$ component (0.68 amplitude square), so that its structure is close to that of the 2^+ state in column (d). This finding is in agreement with the results of Arora *et al.* [46] who observe a sizable fraction of the (p,p') scattering strength to this state to proceed through its one-phonon component.

Altogether, it turns out that states of band [2] have no definite symmetry character along the isotopic chain.

Finally, we observe that, for each isotope, there is only a limited range of values of ξ_2 which allows us to reproduce

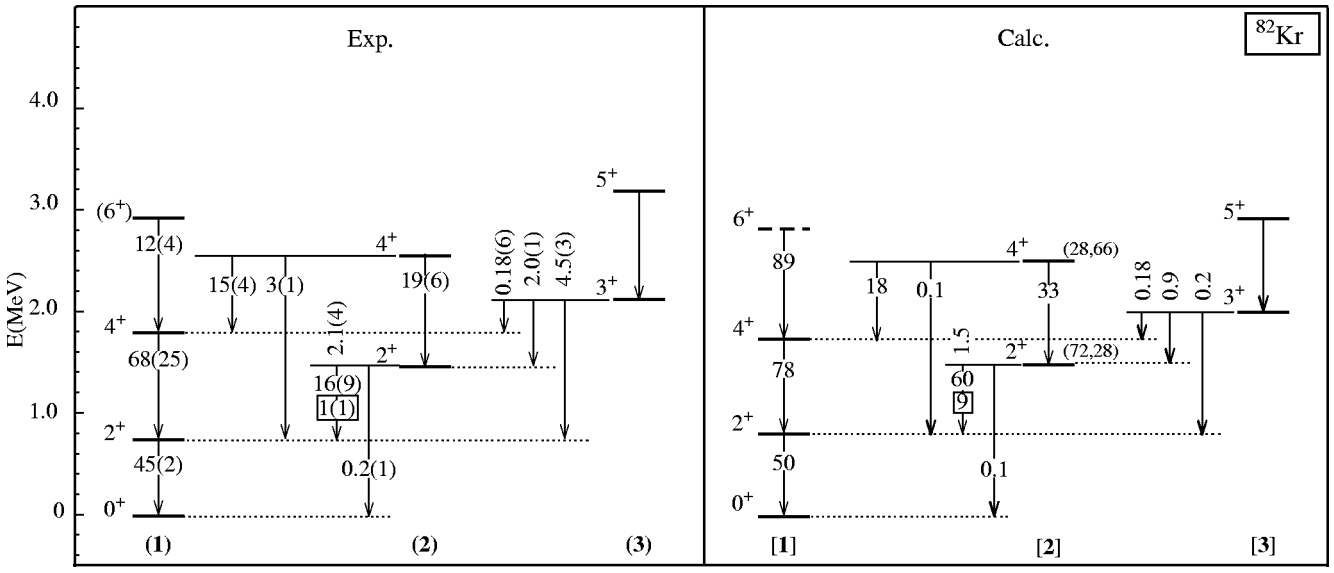

FIG. 9. As in Fig. 6, for ^{82}Kr.

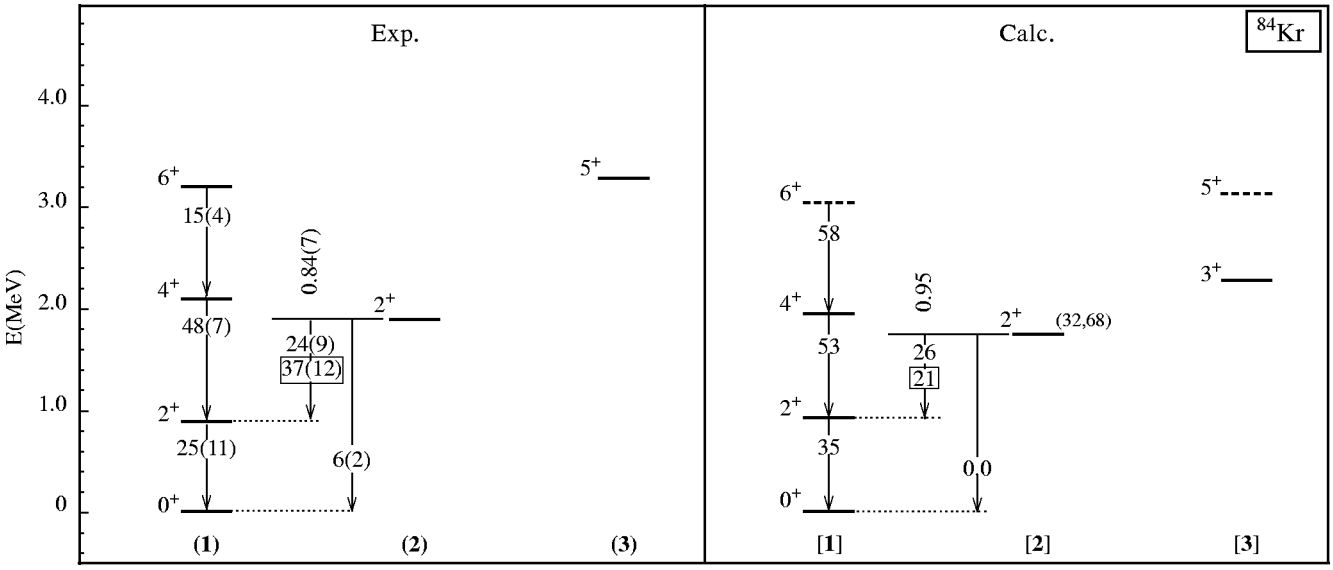

FIG. 10. As in Fig. 6, for ^{84}Kr.

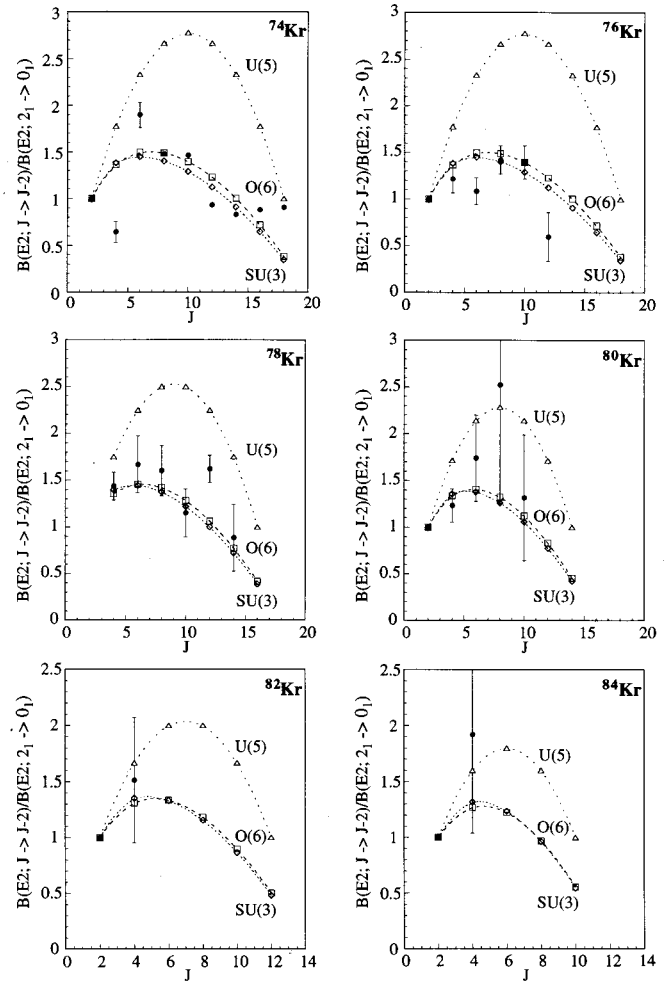

FIG. 11. Experimental ratios $B(E2;J\rightarrow J-2)/B(E2;2_1^+\rightarrow 0_1^+)$ in $^{74-84}$Kr are compared to the predictions of the IBA-2 model for the U(5), O(6), and SU(3) limits.

reasonably well the experimental data and it is mainly this property that has been exploited to fix the value of this parameter.

C. Band (3)

The lowest state of this band has $J^\pi=3^+$. Band (3) has been identified in $^{74-82}$Kr. In ^{84}Kr the association of the calculated 5^+ state to the experimental 5^+ state at 3.259 MeV, based on the comparison of the experimental and calculated energy, can only be considered tentative since no 3^+ state has been observed in this isotope.

The excitation energies of the states of band (3) in each isotope can be successfully reproduced only through a suitable choice of the ξ_2 and ξ_3 values. As an example, in Fig. 12 are reported the energies of band [3] in ^{76}Kr as a function of ξ_3, having kept ξ_2 at the value reported in Table I. For the adopted value of ξ_3 (indicated by the vertical dashed line) the experimental excitation energies are reproduced to better than 2%. A similar agreement is obtained for the other isotopes.

The excitation energies of the states of band (3) are reported in Fig. 13, together with those of band (1), as a function of the mass number. Their general trend does not fit a picture limited to FS states in nuclei having a structure not too far from the O(6) or U(5) limit of the model [3]. In fact, this would imply rather close energies for the pairs of states represented by the same symbol in the figure, whereas this is observed only for the 6^+, 3^+ states in ^{74,76}Kr and the 8^+, 5^+ states in ^{74}Kr.

The $B(E2)$ values of the intraband transitions are known in $^{76-80}$K, where their order of magnitude is the same as in band (1). Their values are well reproduced by the calculations. At the same time, the observed transitions towards states of bands (1) and (2) have small $E2$ components [$B(E2)$ values up to two order of magnitude smaller than

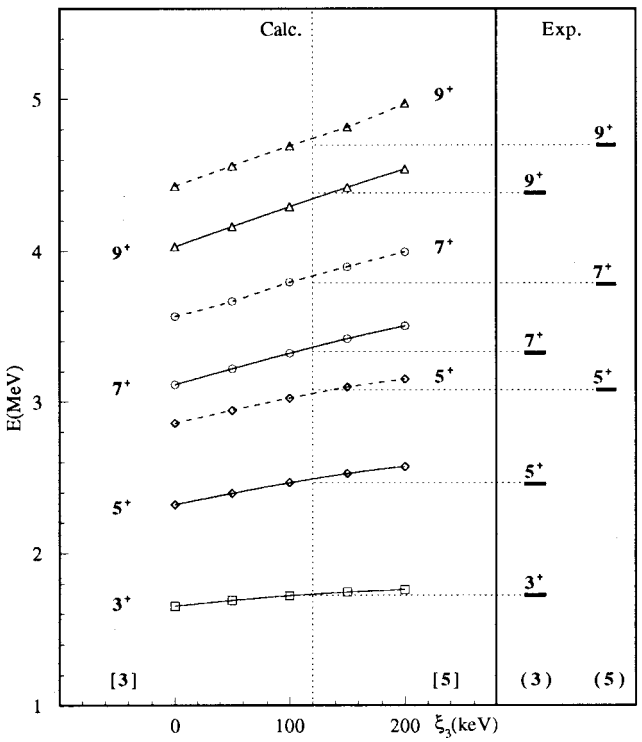

FIG. 12. Excitation energies of bands [3] and [5] in ^{76}Kr as a function of the Majorana parameter ξ_3. The values of the remaining Hamiltonian parameters are those reported in Table I. The corresponding experimental data are reported on the right side of the figure. The vertical dashed line is drawn in correspondence of the adopted value of ξ_3. The predicted energies of the states belonging to band [3] are connected by a full line, those of states of band [5] by a dashed line. The horizontal dotted lines are drawn to help in the comparison between experimental and calculated energies.

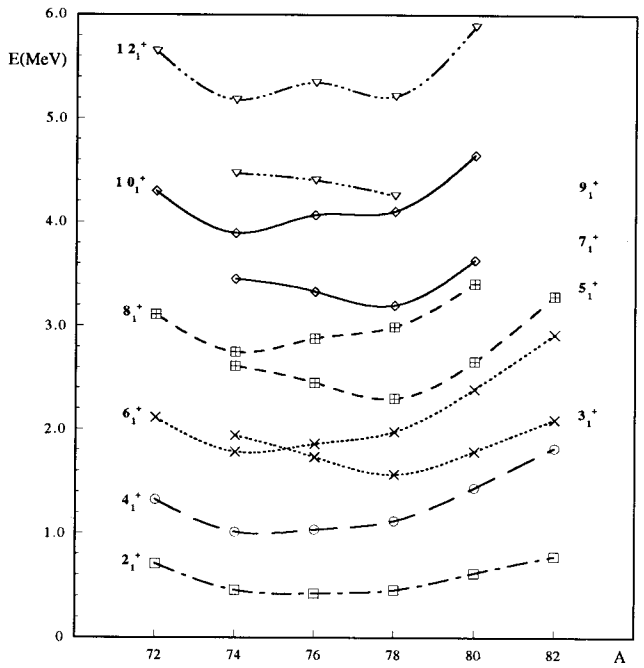

FIG. 13. Energy of the states of band (1) and (3) as a function of the mass number.

those observed in band (1)] and large $M1$ components [see the experimental values of $B(M1)$, $\delta(E2/M1)$ or the predominant $M1$ multipolarity of the relevant transitions in Figs. 5–9].

The capability of the calculations to reproduce the $B(E2)$ values and the predominant $M1$ character of interband transitions rests on the predictions of large MS components for the states of band [3] along the isotopic chain. The decomposition of the wave functions of these states in terms of F-spin and n_d components is reported in Fig. 14 for J up to 9. In each isotope, as J increases, the percentage of the MS components increases and the structure of the states approaches that of the corresponding states in band (e); this is particularly evident in the heavy krypton isotopes. In ^{74,76}Kr the calculations predict two 3^+ states, at an energy close to that of the 6_1^+ state, having a structure similar to that of the 3^+ states of bands (c) and (e), respectively. This gives rise to a mixing of both F-spin and n_d components ($F=F_{max}$ being the largest one for the $[3_1]$ state). Apart from these two states, all states of band [3] have a predominant MS character.

We have already pointed out the existence in heavier ruthenium isotopes of a MS band based on a 3^+ state [17] but in that case the lack of definite spin-parity assignments and of data on the electromagnetic (e.m.) properties of the states of interest prevented us from performing an extended comparison.

D. Bands (4) and (5) in ^{76}Kr

A group of states strongly connected by $\Delta J=1$, dipole transitions has been recently observed by Döring *et al.* [38] in ^{76}Kr. It has been interpreted by these authors as a single band built upon the $4^{(+)}$ state at 2.844 MeV. The structure of this state would be that of a two quasineutron configuration strongly coupled to a large prolate deformation of the core.

We would like to discuss a tentative interpretation of this group of states as belonging to two $\Delta J = 2$ bands having a structure close to that of bands (f) and (g), built on the $4^{(+)}$ state at 2.844 MeV and on the $5^{(+)}$ at 3.095 MeV state, respectively.

In Fig. 6 the experimental states are reported in two separated groups, labeled by numbers (4) and (5). The energies of the states of bands [4] and [5] are very sensitive to the values of ξ_2 and ξ_3. As an example, in Fig. 12 states of band [5] (together with those of band [3] in the same isotope) are reported as a function of ξ_3. They show an approximately linear dependence on ξ_3, with a slope which increases slightly with J (hence with n_d) as expected for states of band (g) (see the expression at the bottom of Fig. 2). In our proposed correspondence, states of band [5] would be the $F_{max}-2$ counterpart of states of band [3] so that their energies should be reproduced for the value of ξ_3 adopted for band [3]. This is indeed the case as appears from the figure: for the indicated value of ξ_3 the agreement between experimental and calculated excitation energies is within $\simeq 1\%$.

As to the energies of states of bands [4], they match those of the experimental ones within $\simeq 4\%$, on the average, for

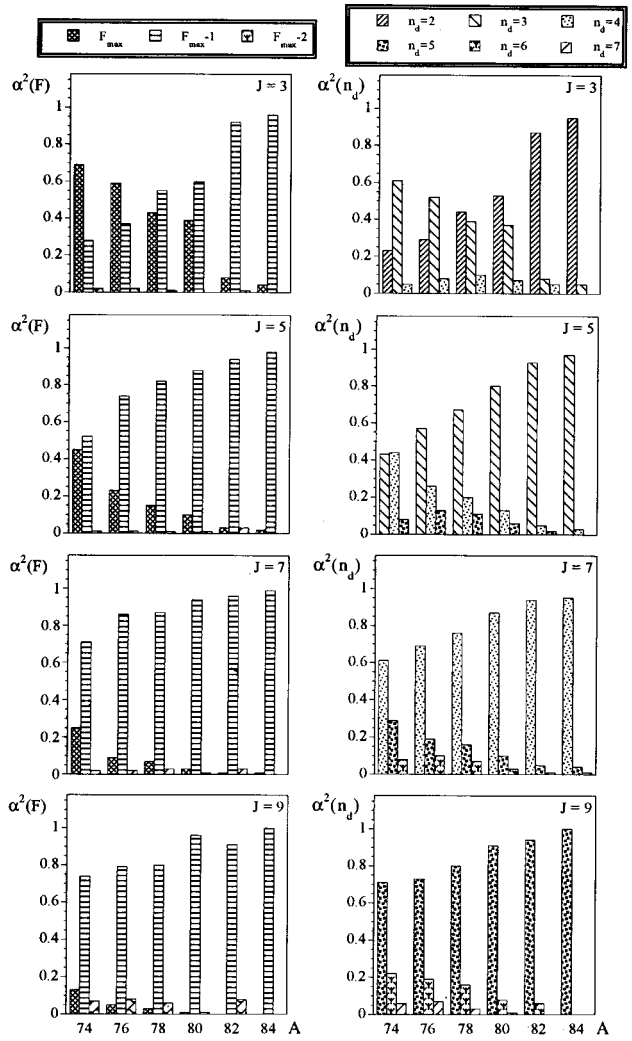

FIG. 14. The three major F-spin and n_d components for the levels of band [3] as a function of the mass number.

the values of the Majorana parameters reported in Table I.

The calculations predict $\Delta J=1$ transitions between states of band [5] and [4] of a quite pure $M1$ character (see the small values of the calculated mixing ratios $E2/M1$). As to the transitions to states of bands [1] and [3], they also are predicted to have an $M1$ component as experimentally observed. It is therefore tempting to associate bands [4] and [5] to the group of states observed in [38].

The F-spin and n_d components of the wave functions of the states of these bands are shown in Fig. 15. Apart from the 4^+ state, which has a strongly mixed structure, the correspondence of bands [4] and [5] with bands (f) and (g), respectively, is quite apparent.

IV. CONCLUSIONS

An analysis of positive-parity bands observed in the even $^{72-84}$Kr isotopes has been carried out in the framework of the IBA-2 model up to the maximum spin allowed by the boson number. The aim was to investigate, on one hand, to what extent their properties could be accounted for (in spite of the significant role that degrees of freedom not included in the model could play) and, on the other hand, whether it was possible to identify bands of definite symmetry in the neutron and proton degrees of freedom, in particular bands of MS character. The U(5) limit of the model has been considered as a starting point for the analysis.

To deduce phenomenologically the parameters of the Hamiltonian we took into account the excitation-energy patterns of the isotopes as well as the e.m. properties of the states. In the analysis, only five out of the 12 parameters present in the Hamiltonian and in the $M1$ and $E2$ transition operators have been varied along the isotopic chain.

The behavior of the Majorana parameters ξ_2, ξ_3 as a function of the neutron number in the Kr chain has been compared to that we found in the Pd and Ru chains.

In krypton isotopes three bands, denoted as bands (1), (2), and (3), have been identified as belonging to the IBA-2

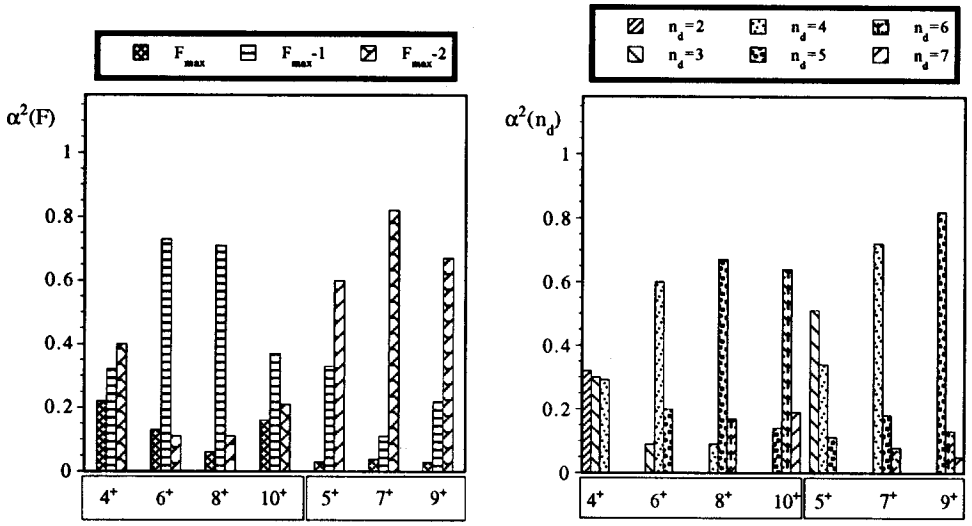

FIG. 15. The three major F-spin and n_d components for the levels of bands [4] and [5] in ^{76}Kr.

model space. The calculations are able to reasonably reproduce the excitation energies, the $B(E2)$ values of intraband transitions, as well as the $B(E2)$ and $B(M1)$ values and the $E2/M1$ mixing ratios of interband transitions.

It turns out that these bands have the following different symmetry characters:

(i) The g.s. band (1) has a predominant FS character. Its properties are quite well reproduced along the isotopic chain; in $^{72-80}$Kr the comparison is successful up to the maximum spin allowed by the total boson number, which in ^{76,78}Kr reaches the value $J=18$.

(ii) Band (2) is built on the 2_2^+ state. In our interpretation the predominant symmetry character can vary among the different members of the same band. This is due to the fact that the calculations predict the existence of two bands built on a $J=2$ state of predominant F_{max} and $F_{max}-1$ character, respectively, in the same energy region.

(iii) Band (3), which has a 3^+ state as the bandhead, has been observed in $^{74-82}$Kr. It has been interpreted as being composed by states having large or predominant $F=F_{max}-1$ components. This finding is particularly interesting because a fully developed band of MS character is clearly identified.

Finally, a tentative interpretation of a group of states strongly connected by $\Delta J=1$, dipole transitions in ^{76}Kr in terms of two MS bands has been suggested.

ACKNOWLEDGMENTS

Many thanks are due to P. G. Bizzeti and A. Gelberg for helpful discussions.

[1] N. Lo Iudice and F. Palumbo, Phys. Rev. Lett. **41**, 1532 (1978); Nucl. Phys. **A326**, 193 (1979).
[2] F. Iachello, Nucl. Phys. **A358**, 89c (1981).
[3] F. Iachello and A. Arima, *The Interacting Boson Model* (Cambridge University Press, Cambridge, England, 1987), and references therein.
[4] D. Bohle, A. Richter, W. Steffen, A.E.L. Dieperink, N. Lo Iudice, F. Palumbo, and O. Scholten, Phys. Rev. Lett. **137B**, 27 (1984).
[5] A. Richter, Prog. Part. Nucl. Phys. **34**, 261 (1995).
[6] U. Kneissl, H.H. Pitz, and A. Zilges, Prog. Part. Nucl. Phys. **37**, 349 (1996).
[7] P.O. Lipas, P. von Brentano, and A. Gelberg, Rep. Prog. Phys. **53**, 1353 (1990), and references therein.
[8] T.F. Fazzini, A. Giannatiempo, A. Nannini, A. Perego, and D. Cutoiu, Z. Phys. A **346**, 21 (1993).
[9] A. Giannatiempo, A. Nannini, P. Sona, and D. Cutoiu, Phys. Rev. C **53**, 2770 (1996).
[10] P.E. Garret, H. Lehmann, C.A. McGrath, Minfang Yeh, and S.W. Yates, Phys. Rev. C **54**, 1 (1996).
[11] N. Pietralla *et al.*, Phys. Rev. C **58**, 796 (1998).
[12] N. Pietralla *et al.*, Phys. Rev. Lett. **83**, 1303 (1999).
[13] A. Giannatiempo, G. Maino, A. Nannini, A. Perego, and P. Sona, Phys. Rev. C **44**, 1508 (1991).
[14] A. Giannatiempo, A. Nannini, A. Perego, and P. Sona, Phys. Rev. C **44**, 1844 (1991).
[15] A. Giannatiempo, A. Nannini, and P. Sona, Phys. Rev. C **58**, 3316 (1998).
[16] A. Giannatiempo, A. Nannini, and P. Sona, Phys. Rev. C **58**, 3335 (1998).
[17] A. Giannatiempo, A. Nannini, P. Sona, and D. Cutoiu, Phys. Rev. C **52**, 2969 (1995).
[18] J.H. Hamilton, P.G. Hansen, and E.F. Zganjar, Rep. Prog. Phys. **48**, 631 (1985).
[19] W. Nazarewicz, J. Dudek, R. Bengtsson, T. Bengtsson, and I. Ragnarsson, Nucl. Phys. **A435**, 397 (1985).
[20] C.J. Gross *et al.*, Nucl. Phys. **A501**, 367 (1989).
[21] J. Döring, V.A. Wood, J.W. Holcomb, G.D. Johns, T.D. Johnson, M.A. Riley, G.N. Sylvan, P.C. Womble, and L.S. Tabor, Phys. Rev. C **52**, 76 (1995).
[22] A. Giannatiempo, A. Nannini, A. Perego, P. Sona, M.J.G. Borge, K. Riisager, O. Tengblad, and ISOLDE Collaboration, Phys. Rev. C **47**, 521 (1993).
[23] U. Kaup and A. Gelberg, Z. Phys. A **293**, 311 (1979).
[24] H. Dejbakhsh, A. Kolomieys, and S. Shlomo, Phys. Rev. C **51**, 573 (1995).
[25] B. Wörmann, K.P. Lieb, R. Diller, L. Lühmann, J. Keinonen, L. Cleemann, and J. Eberth, Nucl. Phys. **A431**, 170 (1984).
[26] H.P. Hellmeister, J. Keinonen, K.P. Lieb, U. Kaup, R. Rascher, R. Ballini, J. Delaunay, and H. Dumont, Nucl. Phys. **A332**, 241 (1979).
[27] R.A. Meyer, J.F. Wild, K. Escola, M.E. Leino, S. Väisälä, K. Forssten, U. Kaup, and A. Gelberg, Phys. Rev. C **27**, 2217 (1983).
[28] I. Talmi, *Simple Models of Complex Nuclei* (Harwood Academic, Switzerland, 1993).
[29] T. Otsuka, N. Yoshida, Program NPBOS Japan Atomic Energy Research Institute Report No. JAERI-M85-094, 1985.
[30] I. Talmi, Phys. Lett. B **405**, 1 (1997).
[31] C. De Coster and K. Heyde, Int. J. Mod. Phys. A **4**, 3665 (1989).
[32] G. de Angelis *et al.*, Phys. Lett. B **415**, 217 (1997).
[33] A.R. Farhan, Nucl. Data Sheets **74**, 532 (1995).
[34] D. Rudolph *et al.*, Phys. Rev. C **56**, 98 (1997).
[35] A. Algora *et al.*, Phys. Rev. C **61**, 031303 (2000).
[36] Balraj Singh, Nucl. Data Sheets **74**, 63 (1995).
[37] J. Döring, G.D. Johns, R.A. Kaye, M.A. Riley, S.L. Tabor, and P.C. Womble, Phys. Rev. C **52**, R2284 (1995).
[38] J. Döring, G.D. Johns, R.A. Kaye, M.A. Riley, S.L. Tabor, and J.X. Saladin, Phys. Lett. B **381**, 40 (1996).
[39] S. Rab, Nucl. Data Sheets **63**, 1 (1991).
[40] H. Sun *et al.*, Phys. Rev. C **59**, 655 (1999).
[41] Balraj Singh, Nucl. Data Sheets **66**, 623 (1992).
[42] M.M. King and W.T. Chou, Nucl. Data Sheets **76**, 285 (1995).
[43] P. Kemnitz, P. Ojeda, J. Döring, L. Funke, L.K. Kostov, H. Rotter, E. Will, and G. Winter, Nucl. Phys. **A425**, 493 (1984).
[44] J.K. Tuli, Nucl. Data Sheets **81**, 331 (1997).
[45] K.S. Krane and R.M. Steffen, Phys. Rev. C **2**, 724 (1970).
[46] B.K. Arora, D.K. Olsen, P.J. Riley, and C.P. Browne, Phys. Rev. C **10**, 2301 (1974).